Nitrite reduction by a pyridinediimine complex with a proton-responsive secondary coordination sphere

Yubin M. Kwon,[a] Mayra Delgado,[a] Lev N. Zakharov,[b] Takele Seda,[c] and John D. Gilbertson[*a]

[a]Department of Chemistry, Western Washington University, Bellingham, Washington 98225, United States

[b]Department of Chemistry, University of Oregon, Eugene, Oregon 97403, United States

[a]Department of Physics, Western Washington University, Bellingham, Washington 98225, United States

Table of Contents	**Page**

Experimental

General considerations. All manipulations were performed using standard Schlenk techniques and/or utilizing an MBraun glovebox (N_2) equipped with a cold well. All reagents were purchased from commercial sources and used as received with the exception of *N,N*-diethylethylenediamine, which was distilled immediately before use. The asymmetric PDI ligand [(ArN=C(CH_3))C_2H_3N((CH_3)C=O] (Ar = 2,6 = ^{i}Pr-C_6H_3) was synthesized according to literature procedures.[1] All solvents were dried and deoxygenated with PureSolv solvent purification system (CuO and alumina columns). Carbon monoxide (99.3%) was purchased from Airgas, Inc. Infrared Spectra were recorded on a Thermo Scientific Nicolet iS10 FT-IR spectrometer equipped with an ATR accessory. ^{1}H and ^{13}C NMR were recorded on a Unity Inova 500 MHz and Mercury Plus 300 MHz FT-NMR Spectrometers. Data are reported in ppm from the solvent resonance as the internal standard unless otherwise noted. Mass spectrometry was recorded on a Varian CP38—GC with Saturn 2000 Ion-Trap (70eV). UV-Vis absorbance data were acquired using a Jasco UV-Vis/NIR spectrometer in a 1 cm quartz cuvette purchased from Starna Cells, Inc. Elemental analyses were performed by ALS (formerly Columbia Analytical Services) in Tuscon, AZ. Electronic paramagnetic resonance (EPR) spectra were recorded using a Bruker EMX spectrometer equipped with an ER041XG microwave bridge, an Oxford Instrument liquid-helium quartz cryostat, and a dual mode cavity (ER4116DM). Solution magnetic susceptibilities were calculated from Evan's method NMR measurements.[2] Solid-phase magnetic susceptibilities were recorded on a Johnson Matthey MSB-1 magnetic susceptibility balance that was calibrated with $HgCo(SCN)_4$. Diamagnetic correction factors were calculated from Pascal's constants.[3]

Electrochemistry. Cyclic voltammetry was carried out using a Pine WaveNow potentiostat employing a standard three-electrode electrochemical cell consisting of a glassy carbon working electrode, platinum auxiliary electrode and a $Ag/AgNO_3$ reference electrode with a vycor tip filled with acetonitrile. All potentials were internally referenced to the ferrocene redox couple. Unless otherwise noted, experiments were carried out under N_2 at room temperature using solutions of 0.001 M analyte with 0.100 M tetra(n-butyl)ammonium hexafluorophosphate ($TBAPF_6$). All reversibility studies were carried out at 50, 100, 150, 200 and 250 mV/s.

p*K*a Determination. p*K*a values in acetonitrile were determined by NMR spectroscopy and are the average of three self-consistent trials. In a typical experiment, a CD_3CN solution of 0.0159 mmol of [Fe(H^{DEA}PDI)(CO)$_2$][PF_6] (**3**) was combined with a CD_3CN solution of 0.0159 mmol of triethylamine (pK_a = 18.82 in acetonitrile) in an NMR tube and allowed to equilibrate for 60 min. The equilibrium populations were determined by NMR, and the equilibrium concentration was determined from the chemical shift, using the equation $\chi_A = (\delta_{eq} - \delta_B)/(\delta_A - \delta_B)$, where χ_A is the mole fraction of the conjugate acid, and δ refers to the measured chemical shift of a given peak

at equilibrium (eq) and for pure samples of the conjugate acid (A) and base (B). Once the equilibrium concentrations were obtained, the pKa value was calculated utilizing Hess's law.

Mössbauer spectra. Mössbauer spectra were recorded at room temperature with a constant-acceleration spectrometer (Wissel GMBH, Germany) in a horizontal transmission mode using a 50 mCi ^{57}Co source. Approximately 0.080 g of sample was crushed in Mössbauer sample holder and drop of Paratone-N was used to cover the sample to prevent oxidation. Data acquisition varied from 2 days to 4 days to get a statistically reasonable spectrum for each sample for analysis. The velocity scale was normalized with respect to a metallic iron at room temperature; hence, all isomer shifts were recorded relative to metallic iron. The Mössbauer spectra were fitted by assuming Lorentzian line shapes using the NORMOS (Wissel GMBH) least-squares fitting program. The isomers and quadrupole splitting parameters were determined from the fitted spectra.

Gas Chromatography. Gas Chromatography was performed on a SRI 8610c GC using either a 6 foot 13x molecular sieve column (CO detection) or a 6 foot HayeSep D column (CO_2 deection) and a TCD detector. Calibration curves and analyses were performed through on-column injection by use of gastight syringes from Hamilton. Varying volumes of pure carbon monoxide or pure Carbon dioxide were injected to construct calibration curves. For headspace samples, a volume of nitrogen equivalent to the sample volume was first injected into headspace. The syringe was then purged thoroughly, after which the sample was drawn up and then injected into the GC.

X-ray Crystallography. Diffraction intensities were collected at 173 K on a Bruker Apex2 CCD diffractometer using MoKα (**1**, **2**) and CuKα (**3**, **4**) radiations, λ= 0.71073 Å and λ= 1.54178 Å, respectively. Absorption corrections were applied by SADABS[4]. Space group was determined based on systematic absences and intensity statistics (**1** and **4**). Structures were solved by direct methods and Fourier techniques and refined on F^2 using full matrix least-squares procedures. All non-H atoms were refined with anisotropic thermal parameters. All H atoms in **1** were found from the residual density map and refined with isotropic thermal parameters without any restrictions. checkCif indicated that one H-C-H angle is 99 degrees and out from the ideal tetrahedral 109.45. Some geometry of the H atoms is not perfect, but getting H atoms from diffraction data are much more important in this case to confirm the composition than to treated H atoms in the calculated positions to avoid this violation B. H atoms in **2**, **3** and **4** were treated in calculated positions in a rigid group model expect the H atom at N atom in **3** involved in H-bonds which was found from the residual density map and refined without restrictions. It should be mentioned that the real orientation of H atoms in the terminal C(9) methyl group in **3** seems to be different versus the positions calculated based on a rigid group model. For the H atom treatment used for **3** there is a short H…H contact (around 1.78 Å) between H atoms in terminal –CH3 and –CH2 groups. It is clear that real positions of the H atoms in the methyl group should

be different to avoid such short H..H contacts, but we could not find the correct positions of H atom in this terminal C(9) Me group. Solvent molecule CH_2Cl_2 in **2** is highly disordered around an inversion center and was treated be SQUEEZE [5]. The correction of the X-ray data is 90 electron/cell; the required value is 84 electron/cell for two solvent molecules in the full unit cell. All calculations were performed by the Bruker SHELXL-2013 package [6].

Crystallographic Data for [Fe(H^{DEA}PDI)(Br)$_2$][Br] (**1**): $C_{29}H_{44}Br_3FeN_5$, M = 758.27, 0.16 x 0.15 x 0.12 mm, T = 173(2) K, Triclinic, space group P-1, a = 10.0331(9) Å, b = 13.3181(12) Å, c = 14.1000(13) Å, α = 64.813(3)°, β = 81.091(2)°, γ = 81.046(2)°, V = 1675.9(3) Å^3, Z = 2, D_c = 1.503 Mg/m^3, μ(Mo) = 4.052 mm^{-1}, $F(000)$ = 768, $2\vartheta_{max}$ = 56.0°, 32196 reflections, 8179 independent reflections [R$_{int}$ = 0.0770], R1 = 0.0403, wR2 = 0.0591 and GOF = 1.007 for 8179 reflections (519 parameters) with I>2σ(I), R1 = 0.0696, wR2 = 0.0893 and GOF = 1.007 for all reflections, max/min residual electron density +0.471/-0.447 eÅ^{-3}.

Crystallographic Data for Fe(^{DEA}PDI)(CO)$_2$ (**2**): $C_{29.5}H_{41}ClFeN_4O_2$, M = 574.96, 0.32 x 0.23 x 0.11 mm, T = 173 K, Monoclinic, space group $P2_1/c$, a = 9.6385(9) Å, b = 13.7609(13) Å, c = 23.410(2) Å, β = 92.164(2)°, V = 3102.7(5) Å^3, Z = 4, D_c = 1.231 Mg/m^3, μ(Mo) = 0.603 mm^{-1}, $F(000)$ = 1220, $2\vartheta_{max}$ = 56.0°, 35837 reflections, 7488 independent reflections [R$_{int}$ = 0.0573], R1 = 0.0434, wR2 = 0.1046 and GOF = 1.065 for 7488 reflections (325 parameters) with I>2σ(I), R1 = 0.0659, wR2 = 0.1113 and GOF = 1.065 for all reflections, max/min residual electron density +0.413/-0.408eÅ^{-3}.

Crystallographic Data for [Fe(H^{DEA}PDI)(CO)$_2$][PF$_6$] (**3**): $C_{29}H_{41}F_6N_4O_2P$, M = 678.48, 0.14 x 0.12 x 0.10 mm, T = 173 K, Monoclinic, space group $P2_1/c$, a = 21.0286(15) Å, b = 8.7204(7) Å, c = 17.6555(12) Å, β = 99.237(5)°, V = 3195.6(4) Å^3, Z = 4, D_c = 1.410 Mg/m^3, μ(Cu) = 4.857 mm^{-1}, $F(000)$ = 1416, $2\vartheta_{max}$ = 135.35°, 27682 reflections, 5641 independent reflections [R$_{int}$ = 0.0980], R1 = 0.0647, wR2 = 0.1394 and GOF = 1.008 for 5641 reflections (392 parameters) with I>2σ(I), R1 = 0.1132, wR2 = 0.1614 and GOF = 1.008 for all reflections, max/min residual electron density +0.501/-0.654 eÅ^{-3}.

Crystallographic Data for [Fe(^{DEA}PDI)(NO)$_2$][PF$_6$] (**4**): $C_{27}H_{40}F_6FeN_6O_2P$, M = 681.47, 0.14 x 0.11 x 0.05 mm, T = 173(2) K, Triclinic, space group P-1, a = 8.4876(5) Å, b = 12.8367(7) Å, c = 16.0181(9) Å, α = 112.855(4)°, β = 90.918(4)°, γ = 99.918(4)°, V = 1578.52(16) Å^3, Z = 2, D_c = 1.434 Mg/m^3, μ(Cu) = 4.937 mm^{-1}, $F(000)$ = 710, $2\vartheta_{max}$ = 133.1°, 20827 reflections, 5531 independent reflections [R$_{int}$ = 0.0660], R1 = 0.0610, wR2 = 0.1730 and GOF = 1.010 for 5531 reflections (388 parameters) with I>2σ(I), R1 = 0.0799, wR2 = 0.1852 and GOF = 1.010 for all reflections, max/min residual electron density +0.648/-0.495 eÅ^{-3}.

Preparation of [(2,6-^{i}Pr-C$_6$H$_3$)N=CMe)(N-C$_4$H$_{10}$-NC$_2$H$_4$)N=CMe)C$_5$H$_3$N] (^{DEA}PDI**).** To an oven-dried 100 mL round bottom flask, equipped with a Dean-Stark apparatus,

[(ArN=C(CH₃))C₂H₃N((CH₃)C=O) (Ar = 2,6 - ^{i}Pr-C₆H₃)] (0.500 g, 1.55mmol) was added with a slight excess of *N,N*-Diethylethylenediamine (0.270 g, 2.32 mmol) and catalytic amount of p-toluenesulfonic acid monohydrate (0.0250 g). The mixture was dissolved with dry toluene (35 mL). The solution was stirred and refluxed at 120 °C for 12 h followed by removal of the toluene. Acetonitrile (5-10 mL) was added to the resulting oil to precipitate out a tan solid. The mixture was filtered through a Büchner funnel and washed with dry acetonitrile yielding a pale tan solid identified as ^{DEA}**PDI**. Yield: 65% (0.421g, 1.00 mmol). FTIR (solid): 1643 cm^{-1}(C=N). ^{1}H NMR (300 mHz, CDCl₃): δ 8.34 (d, 1H), 8.16 (d, 1H), 7.70 (t, 1H), 7.15 (m, 3H), 3.69 (t, 2H), 2.91 (t, 2H), 2.70 (m, 6H), 2.44 (s, 3H), 2.24 (s, 3H), 1.16 (d, 12H), 1.09 (d, 6H). ^{13}C NMR (300 mHz, CDCl₃): δ 166.1, 155.4, 153.7, 145.4, 135.6, 134.8, 122.4, 121.9, 120.7, 120.3, 52.5, 50.3, 46.6, 27.2, 22.1, 21.8, 16.1, 12.9, 10.8. GCMS (M$^+$) *m/z* calculated for C₂₇H₄₀N₄: 420.3 Found: 421.3 [M+H].

Preparation of [Fe(H^{DEA}PDI)Br₂][Br] (1). In a 20 mL scintillation vial equipped with a stir bar, ^{DEA}PDI (0.100 g, 0.238 mmol)) was dissolved in 10 mL THF producing a tan orange solution. While stirring, FeBr₂ (0.051 g, 0.238 mmol) was added to the solution instantly producing a blue color. The solution was allowed to stir overnight. The solvent was removed *in vacuo*, yielding a blue solid. The solid was redissolved with approximately 5 mL of CH₃CN and then filtered through a pipette packed with glass wool and celite into a scintillation vial. The filtrate was layered with diethyl ether and the vial was set aside for 1 day, after which blue crystals of **1** were isolated. Yield: 65% (0.117 g, 0.154 mmol, calculated based on C₂₉H₄₄FeN₅Br₃, see below). FTIR (solid): 3399cm^{-1}(N-H); 1612, 1584 cm^{-1} (C=N). ^{1}H NMR (500 mHz, CD₂Cl₂): δ -35.36, -15.10, -9.66, -1.31, -0.73, -0.36, 0.90, 1.18, 1.28, 2.05, 3.45, 4.31, 5.35, 77.84, 79.63, 139.36. Evan's Method: μ$_{eff}$: 4.68 μ$_B$ (solution), 4.64 μ$_B$ (solid). ^{57}Fe Mossbauer: δ = 0.787(6) mms^{-1}; ΔE = 1.57(1) mms^{-1}. Anal calcd for C₂₇H₄₁FeN₄Br₃: C, 45.22; H, 5.76; N, 7.81; Found: C, 45.90; H, 5.95; N, 8.63. The discrepancy in calc vs found can be attributed to acetonitrile solvent of crystallization. See X-ray structure.

Preparation of Fe(^{DEA}PDI)(CO)₂ (2). An 88 mL Fisher-Porter tube was charged with compound **1** (0.200 g, 0.279 mmol), sodium mercury amalgam (0.578 g, 5%Na), a stir bar, and approximately 10 mL of methylene chloride were added to the tube. The tube was closed with a pressure valve and charged with 20 psi of CO and left to stir vigorously overnight. The solvent was then removed *in vacuo* and brought back in to the glove box to be re-dissolved in diethyl ether and filtered through a pipette packed with glass wool and celite. Slow evaporation of the diethyl ether resulted green crystals identified as **2** (70%). IR (solid): 1934, 1872 cm^{-1}(C=O). ^{1}H NMR (500 mHz, CD₂Cl₂): δ 7.95 (d, 1H), 7.91 (d, 1H), 7.39 (t, 1H), 7.17 (m, 3H), 4.23 (t, 2H), 2.73 (t, 2H), 2.60 (s, 3H), 2.50 (q, 4H), 2.37 (sept, 2H), 2.24 (s, 3H), 1.13 (d, 6H), 0.92 (m, 12H). ^{13}C NMR (500 mHz, CD₂Cl₂): δ 216.2 (C=O), 157.2, 157.7, 151.2. 147.1, 145.9, 141.7, 127.4, 124.8, 122.2, 121.3, 118.6, 109.5, 60.8, 56.8, 49.0, 28.6, 25.8, 25.4, 17.7, 15.5, 13.5. ^{57}Fe Mossbauer: δ = -0.081(3) mms^{-1}; ΔE = 1.450(8) mms^{-1}. Anal calcd for C₂₉H₄₀FeN₄O₂: C, 65.41; H, 7.57; N, 10.52; Found: C, 60.95; H,

7.34; N, 9.64.   The discrepancy in calc vs found can be attributed to CH_2Cl_2 solvent of crystallization.   See X-ray structure.

Preparation of [Fe(H^{DEA}PDI)(CO)$_2$][PF$_6$] (3). In a scintillation vial equipped with a stir bar, **2** (0.100 g, 0.188 mmol)) was dissolved in 5 mL CH_2Cl_2 producing a green solution. While stirring, a solution of NH_4PF_6 (0.061 g, 0.374 mmol) dissolved in 3 mL of CH_3OH was added to the drop wise to the solution of **3**. The solution was allowed to stir overnight. The solvent was removed *in vacuo*, yielding a green solid. The solid was redissolved with approximately 5 mL of CH_2Cl_2 and then filtered through celite into a scintillation vial. The filtrate was layered with pentane and the vial was set aside for 1 day, after which dark crystals of **3** (80%). IR (solid): 3189 cm^{-1}(N-H); 1950, 1886 cm^{-1} (C=O); 835 cm^{-1} (PF$_6^-$). ^{1}H NMR (500 mHz, CD_2Cl_2): δ 8.14 (t, 2H), 7.61 (t, 1H), 7.28 (m, 3H), 4.67 (t,2H), 3.50 (t, 3H), 3.39 (s, 3H) 2.72 (s, 3H), 2.48 (sept, 2H), 2.39 (s, 3H), 1.46 (t, 6H), 1.24 (d, 6H), 1.03 (d, 6H). ^{13}C NMR (CD_2Cl_2): δ 216.7 (C=O), 159.8, 158.6, 141.1, 147.42, 147.0, 141.9, 128.3, 125.4, 123.9, 123.3, 120.5, 109.9, 67.5, 50.9, 29.2, 26.2, 25.9, 18.4, 16.9, 16.1, 10.3. ^{57}Fe Mossbauer: δ = -0.07(2) mms^{-1}; ΔE = 0.97(2) mms^{-1}. Anal calcd for $C_{29}H_{41}FeN_4O_2PF_6$: C, 51.43; H, 6.09; N, 8.26; Found: C, 51.51; H, 6.13; N, 8.33.

Preparation of [Fe(^{DEA}PDI)(NO)$_2$][PF$_6$] (4). In a 20 mL scintillation vial equipped with a stir bar, **3** (0.050 g, 0.074 mmol)) was dissolved in 8 mL THF producing a green solution, closed with a fresh septum, and stirred for 30 min. While stirring, a solution of $NaNO_2$ (0.005 g, 0.072 mmol) dissolved in 2 mL of CH_3OH was injected dropwise to the solution of **3**. The solution was allowed to stir overnight. The solution turns from a green to red brown solution. After GC analysis of the headspace, the solvent was removed *in vacuo*, yielding a brown solid. The solid was redissolved with approximately 5 mL of THF and then filtered through a pipette packed with glass wool and celite into a scintillation vial. The filtrate was layered with pentane and the vial was placed in the glovebox freezer for 48 h resulting in purple crystals of **4** (52%). FTIR (ATR): 1786, 1715 cm^{-1} (NO); 831 cm^{-1} (PF$_6^-$). ^{57}Fe Mossbauer: δ = 0.308(7) mms^{-1}; ΔE = 0.89(1) mms^{-1}. Anal calcd for $C_{27}H_{40}FeN_6O_2PF_6$: C, 47.59; H, 5.92; N, 12.33; Found: C, 47.44; H, 5.95; N, 12.04.

Reactivity of 3 with Na^{15}NO$_2$ to form [Fe(^{DEA}PDI)(^{15}NO)$_2$][PF$_6$]. In a scintillation vial equipped with a stir bar, **3** (0.050 g, 0.074 mmol)) was dissolved in 8 mL THF producing a green solution and stirred for 30 min. While stirring, a solution of Na^{15}NO$_2$ (0.005 g, 0.072 mmol) dissolved in 2 mL of CH_3OH was added drop wise to the solution of **3**. The solution was allowed to stir for 3 hours. The solution turns from a green to red brown solution. The solvent was removed *in vacuo*, yielding a brown solid. The solid was redissolved with approximately 1.5 mL of THF and then filtered through a pipette packed with glass wool and celite. The solid was redissolved with approximately 2 mL of THF and then filtered through a pipette packed with glass wool and celite. A slow vapor diffusion of pentane into a THF solution of [Fe(^{DEA}PDI)(^{15}NO)$_2$][PF$_6$] afforded purple crystals. IR (solid): 1744, 1666 cm^{-1} (NO); 830 cm^{-1} (PF$_6^-$).

CoTPP NO trapping experiments. Method A. Under an N_2 atmosphere, 2.5 mL of a stock solution of 7.4 mM CoTPP in THF was added into a 20 mL scintillation vial. Stock solutions of [HEt$_3$N][PF$_6$] in THF, and NaNO$_2$ in MeOH, at concentrations of 7.4 mM were also prepared. In a small 2 mL vial, 0.36 mL of stock NaNO$_2$ and a stir bar was added, and the vial was carefully placed inside the 20 mL of scintillation vial of CoTPP. The 20 mL scintillation vial was then capped with a fresh septum. After 10 min, 0.36 mL of the [HEt$_3$N][PF$_6$] solution was syringed into the small vial containing the NaNO$_2$ solution. After 60 min of stirring, approximately 2.5 mL of the CoTPP solution was syringed out of the 20 mL scintillation vialed and carefully transferred into an injectable quartz cuvette and the UV-Vis spectrum was obtained.

Method B. The experiment described above was repeated except all solutions were mixed in the same 20 mL scintillation vial.
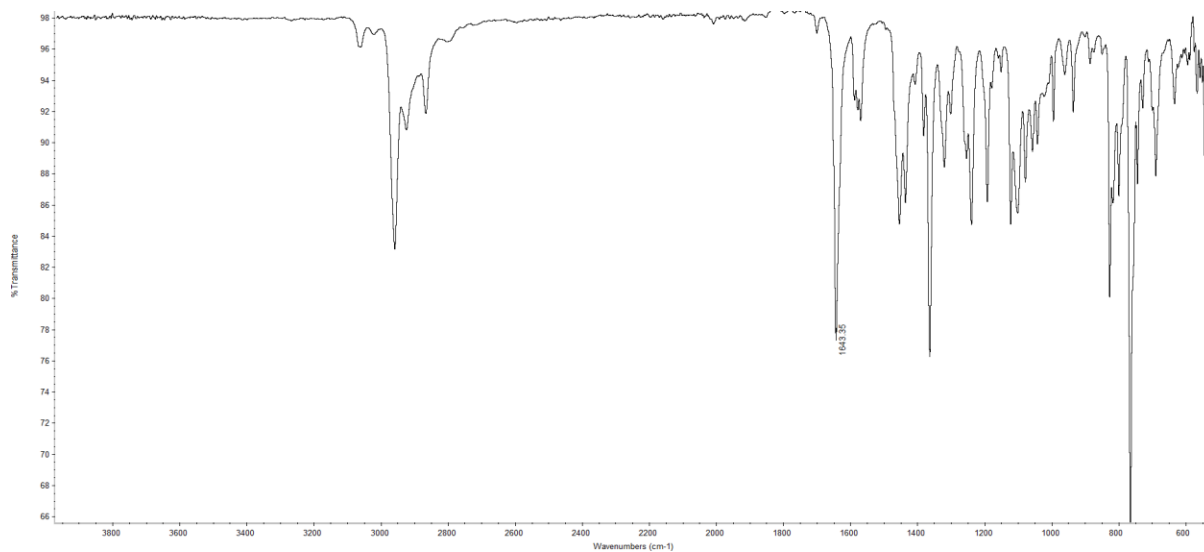
Figure S1. ATR-FT-IR spectrum of ^{DEA}PDI.
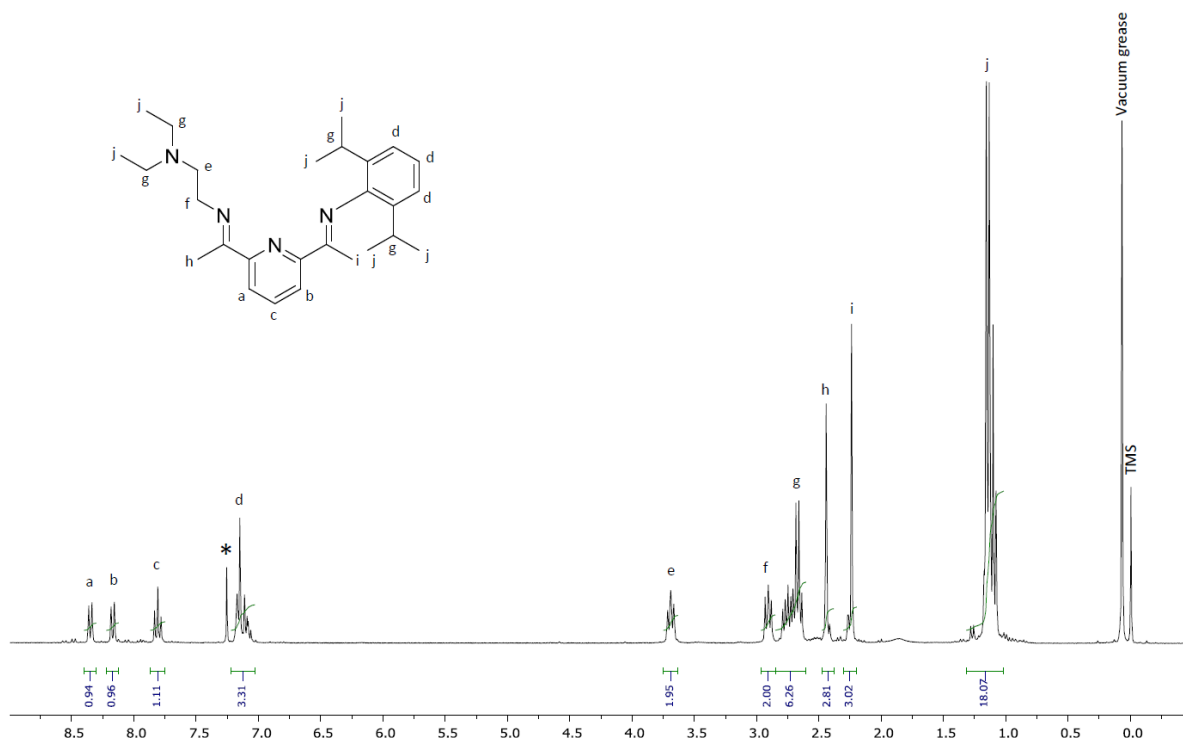
Figure S2. ¹H NMR spectrum of ^{DEA}PDI, 300 MHz, CDCl₃. (* represents solvent)
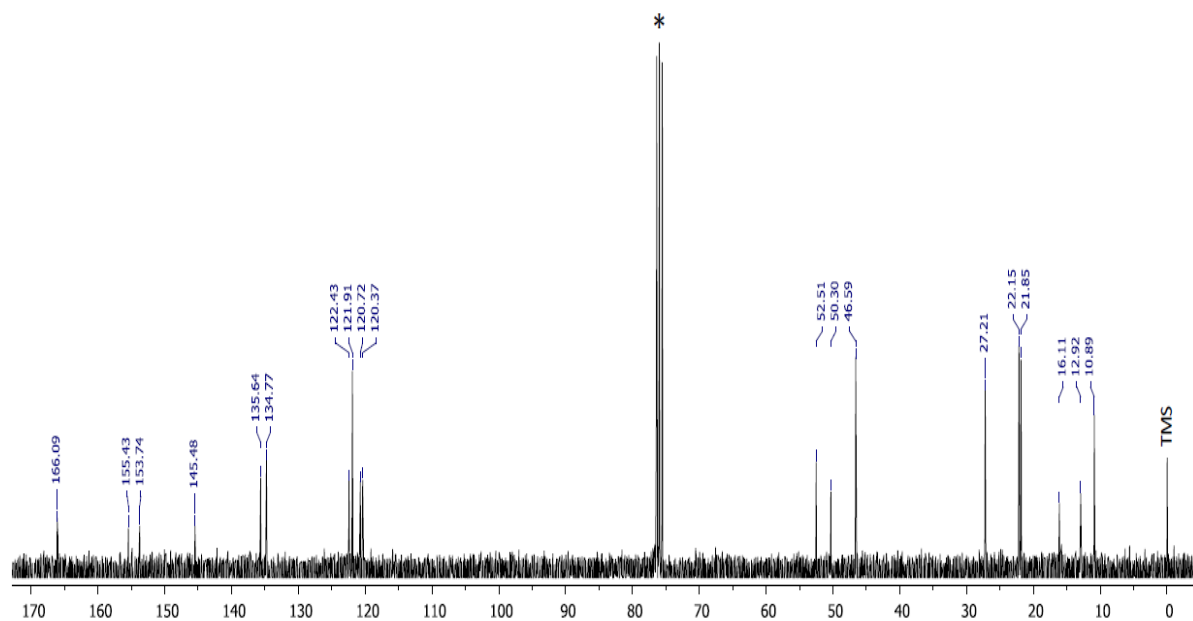
Figure S3. $^{13}C\{^1H\}$ NMR spectrum of ^{DEA}**PDI**, 300 MHz, CDCl$_3$ (* represents solvent).
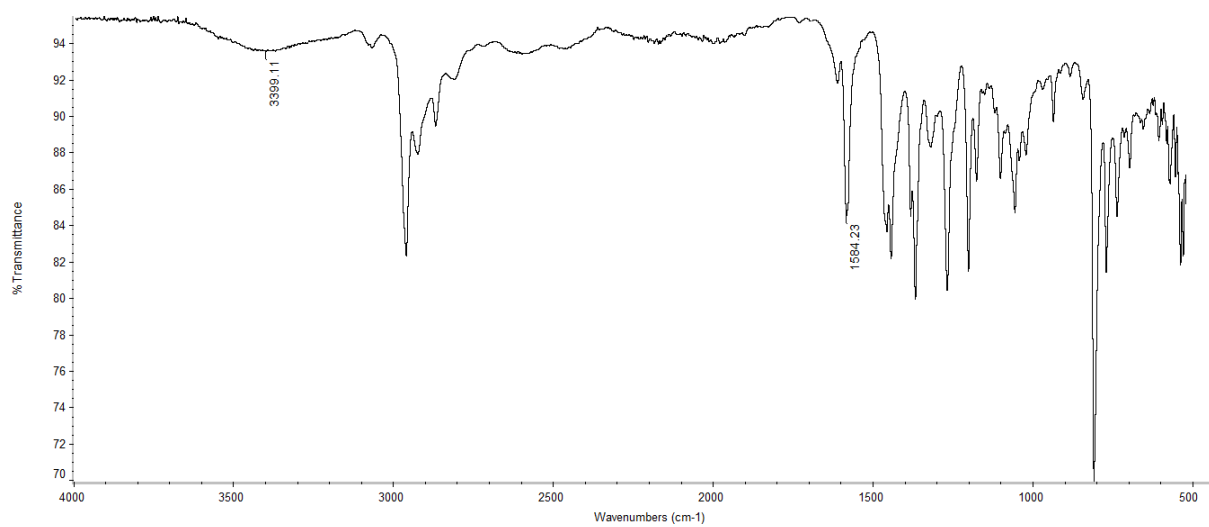
Figure S4. ATR-FTIR spectrum of [Fe(H^{DEA}PDI)Br$_2$][Br] (**1**).
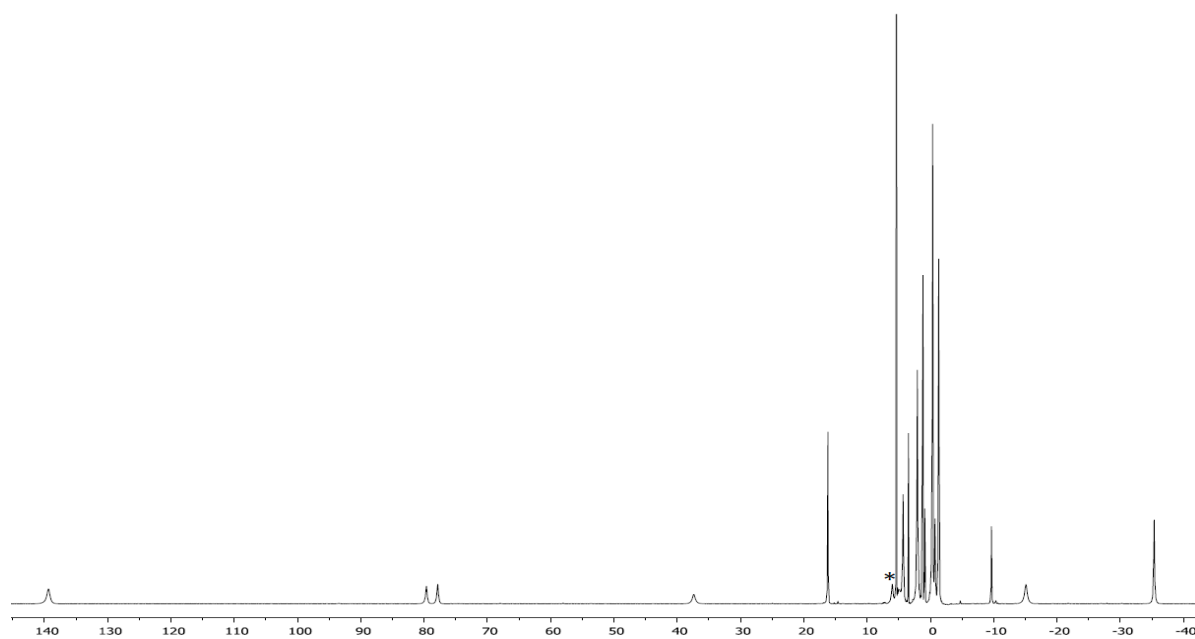
Figure S5. ^{1}H NMR spectrum of [Fe(H^{DEA}PDI)Br$_2$][Br] (**1**), CD$_2$Cl$_2$ (* represents solvent).
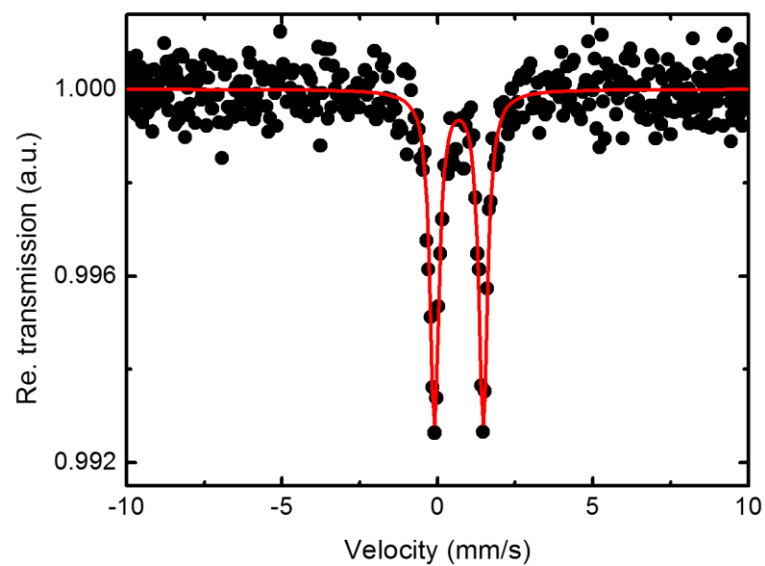
Figure S6. Zero-field Mössbauer spectrum of [Fe(H^{DEA}PDI)Br$_2$][Br] (**1**), [δ = 0.787(6); ΔE_Q = 0.787(6) mm/s].
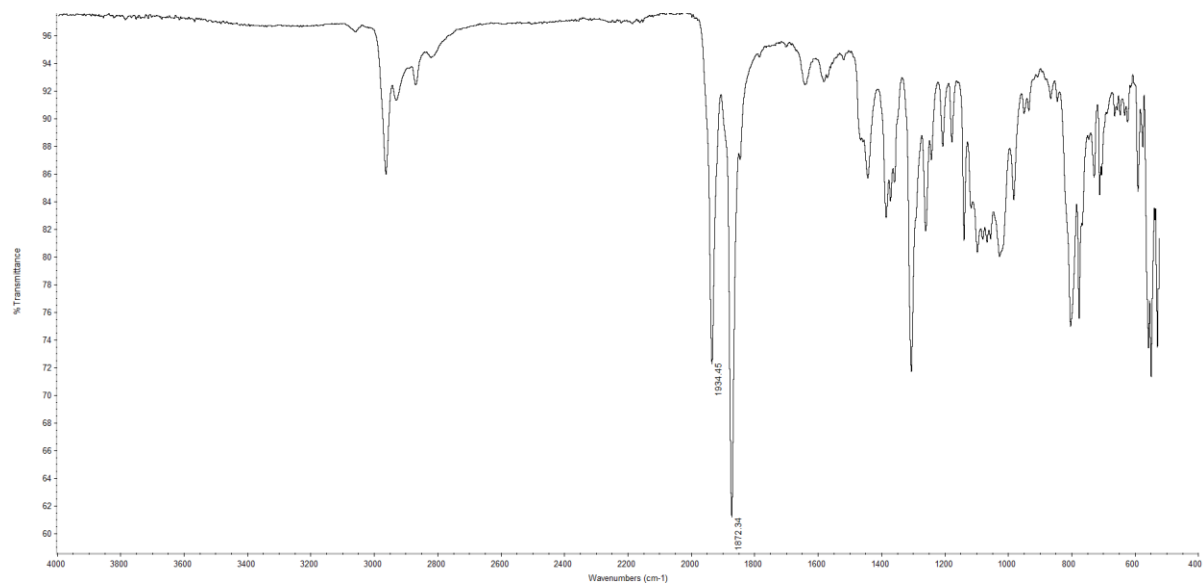
Figure S7. ATR-FTIR spectrum of Fe(^{DEA}PDI)(CO)$_2$ (**2**).
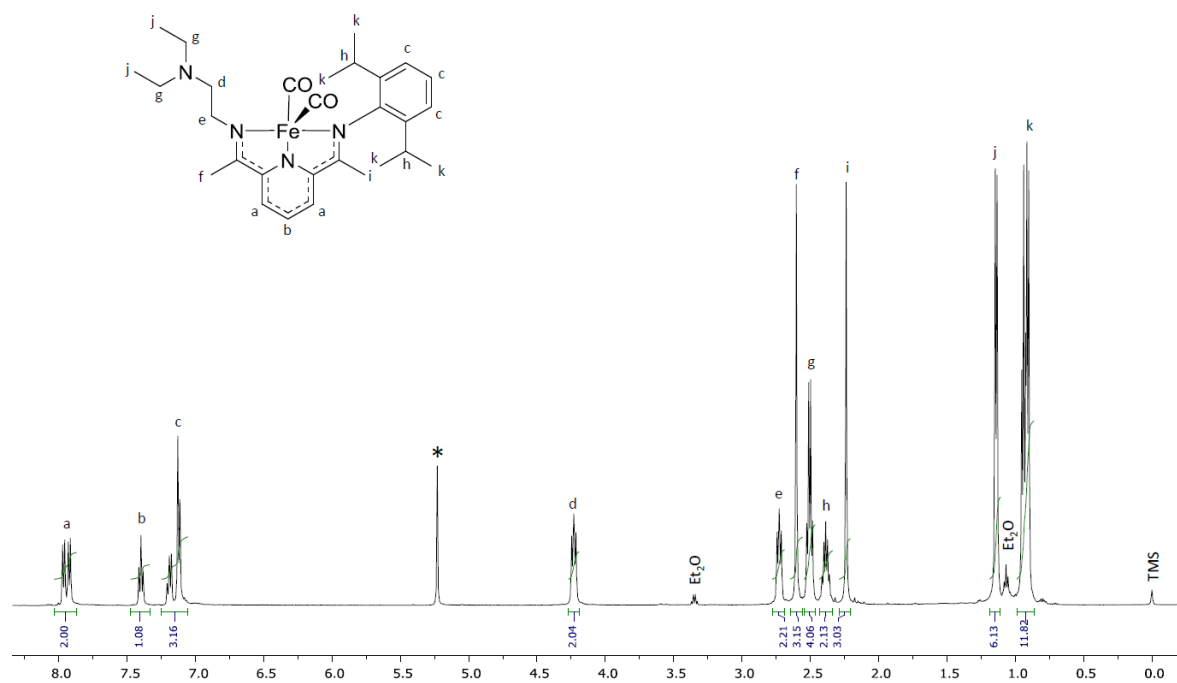
Figure S8. ^{1}H NMR spectrum of Fe(^{DEA}PDI)(CO)$_2$ (**2**), 500 MHz, CD$_2$Cl$_2$. (* represents solvent)
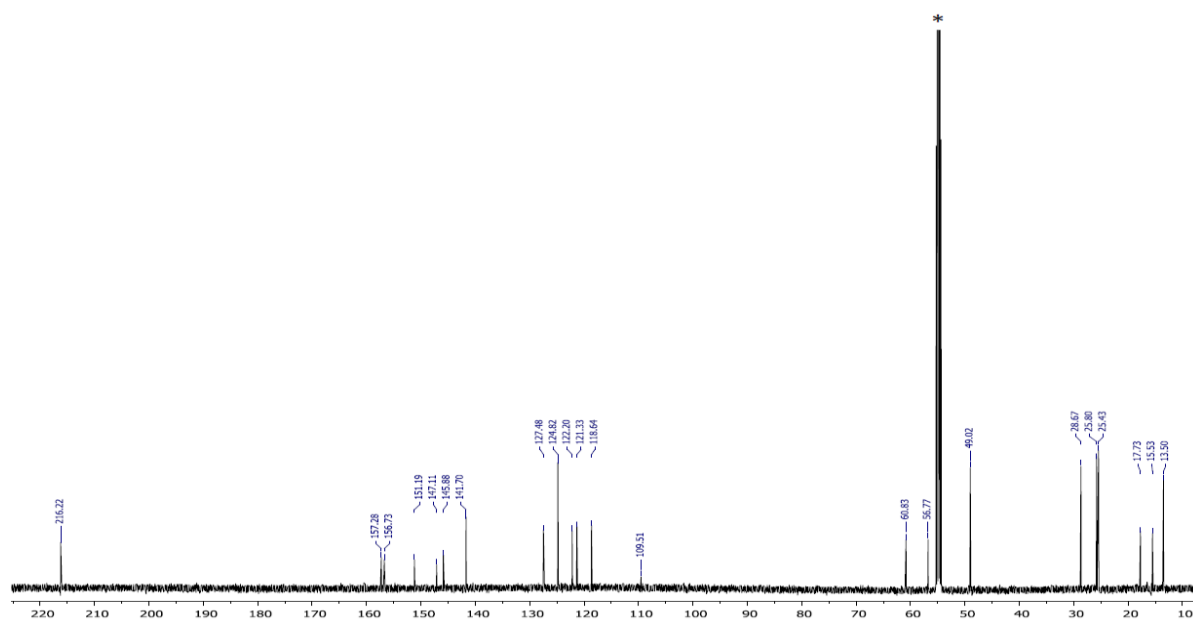
Figure S9. $^{13}C\{^{1}H\}$ NMR spectra of Fe(^{DEA}PDI)(CO)$_2$ (**2**), 500 MHz, CD$_2$Cl$_2$.
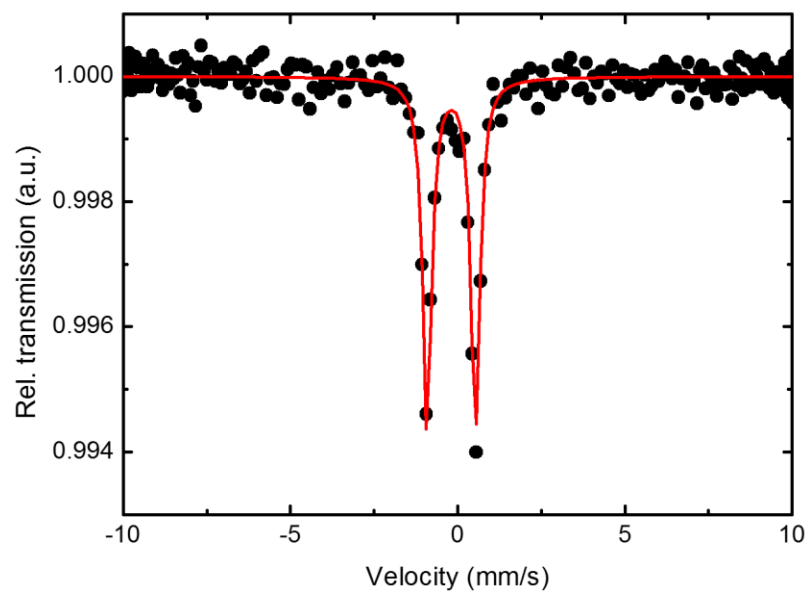
Figure S10. Zero-field Mössbauer spectrum of Fe(^{DEA}PDI)(CO)$_2$ (**2**), [δ = −0.081(3); ΔE_Q = 1.450(8) mm/s].
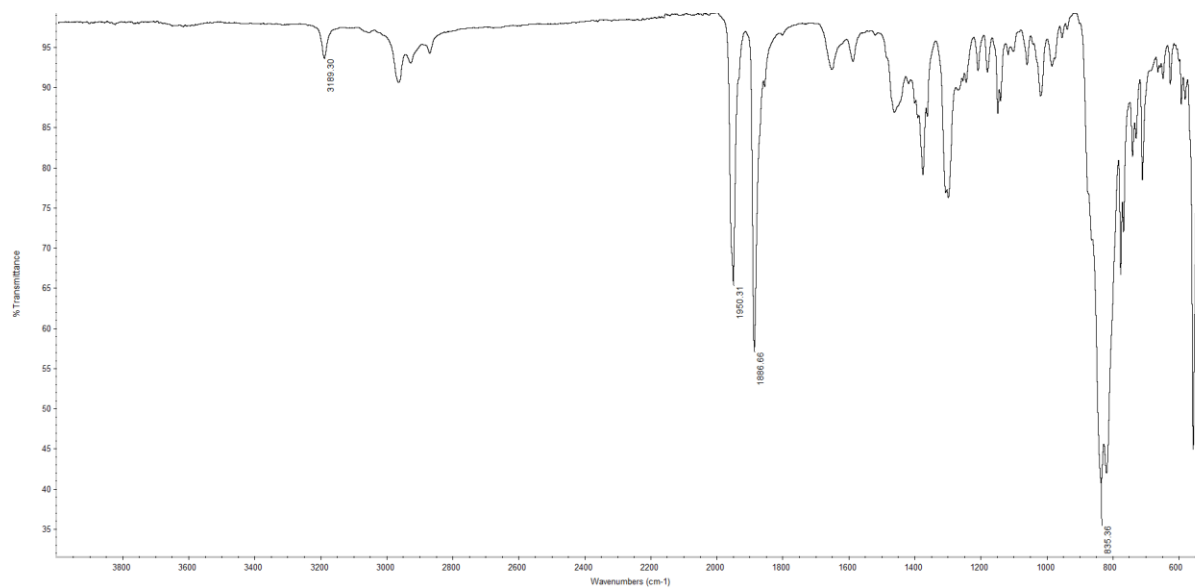
Figure S11. ATR-FTIR spectrum of [Fe(H^{DEA}PDI)(CO)$_2$][PF$_6$] (**3**).
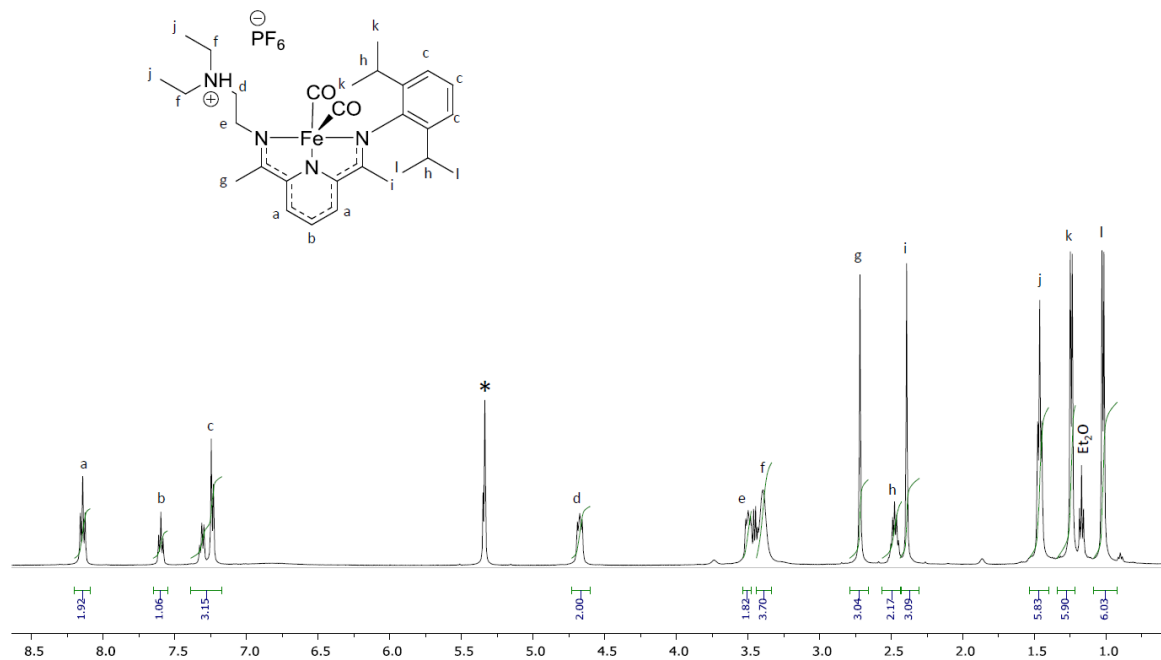
Figure S12. ^{1}H NMR spectrum of [Fe(H^{DEA}PDI)(CO)$_2$][PF$_6$] (**3**), 500 MHz, CD$_2$Cl$_2$. (* represents solvent)
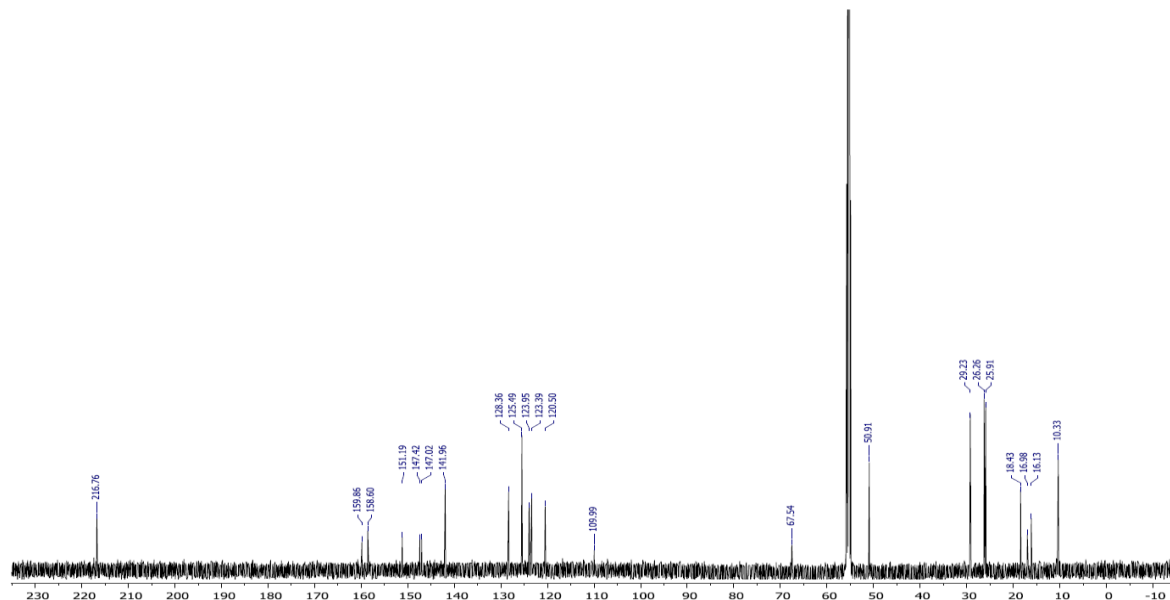
Figure S13. $^{13}C\{^{1}H\}$ NMR spectra of [Fe(H^{DEA}PDI)(CO)$_2$][PF$_6$] (**3**), 500 MHz, CD$_2$Cl$_2$.
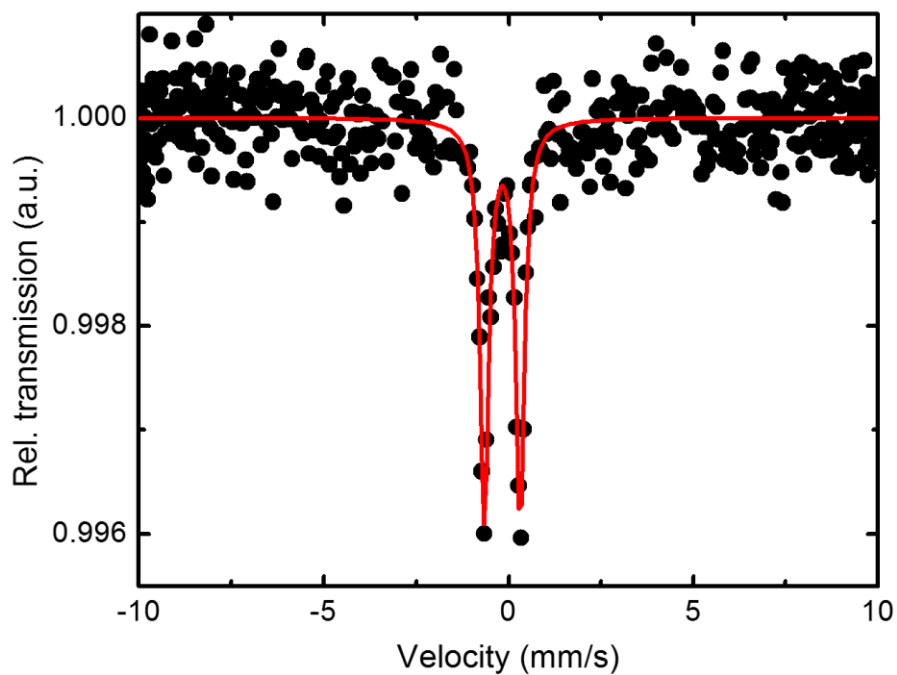
Figure S14. Zero-field Mössbauer spectrum of [Fe(H^{DEA}PDI)(CO)$_2$][PF$_6$] (**3**), [δ = -0.07(2); ΔE_Q = 0.97(2) mm/s].
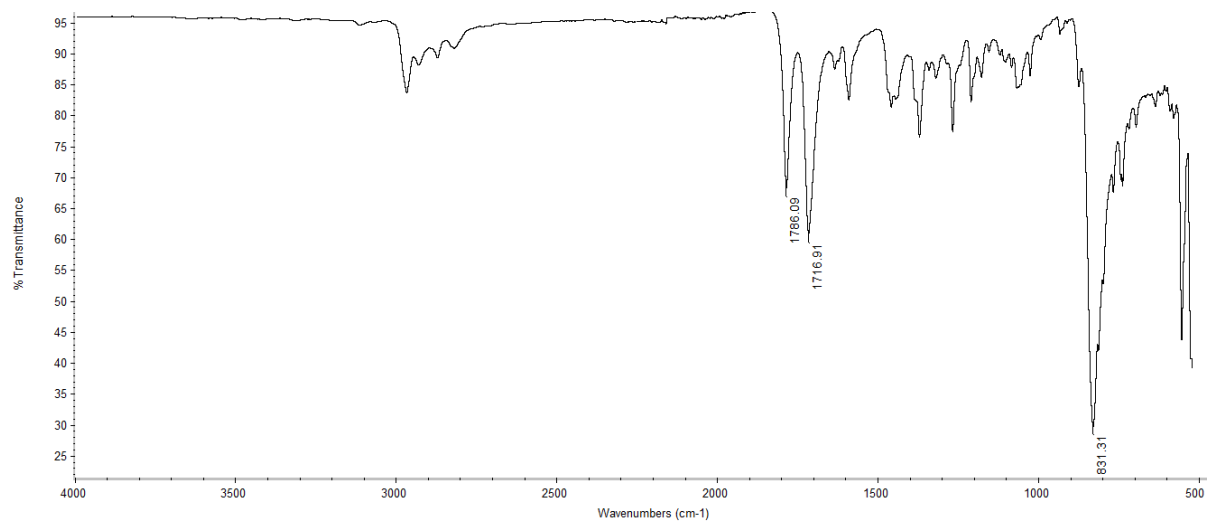
Figure S15. ATR-FTIR spectrum of [Fe(^{DEA}PDI)(NO)$_2$][PF$_6$] (**4**).
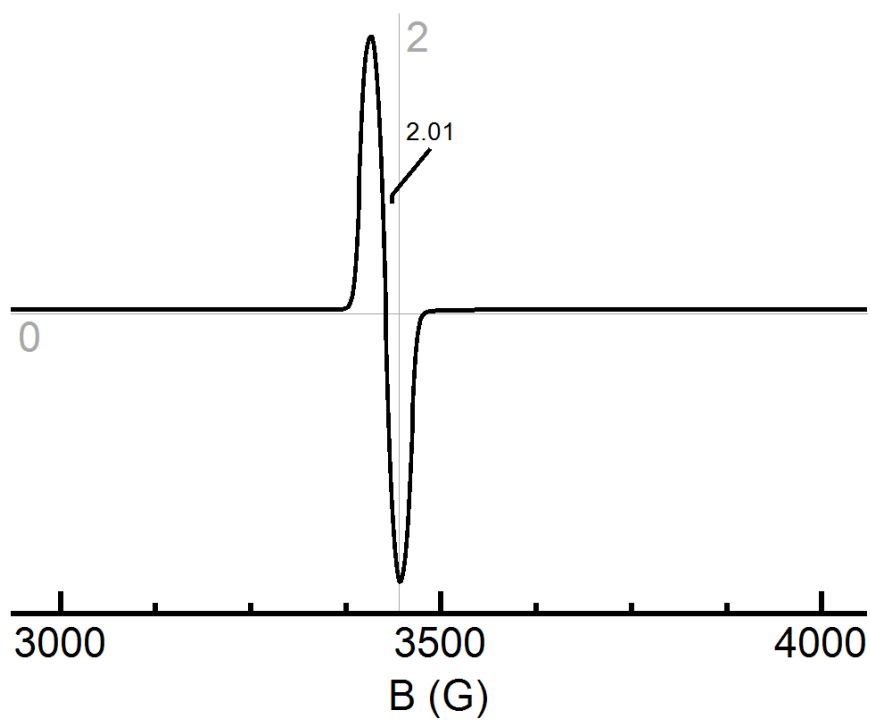
Figure S16. EPR spectra of 1mM solution (THF) of [Fe(^{DEA}PDI)(NO)$_2$][PF$_6$] (**4**) (X-band, 77K).
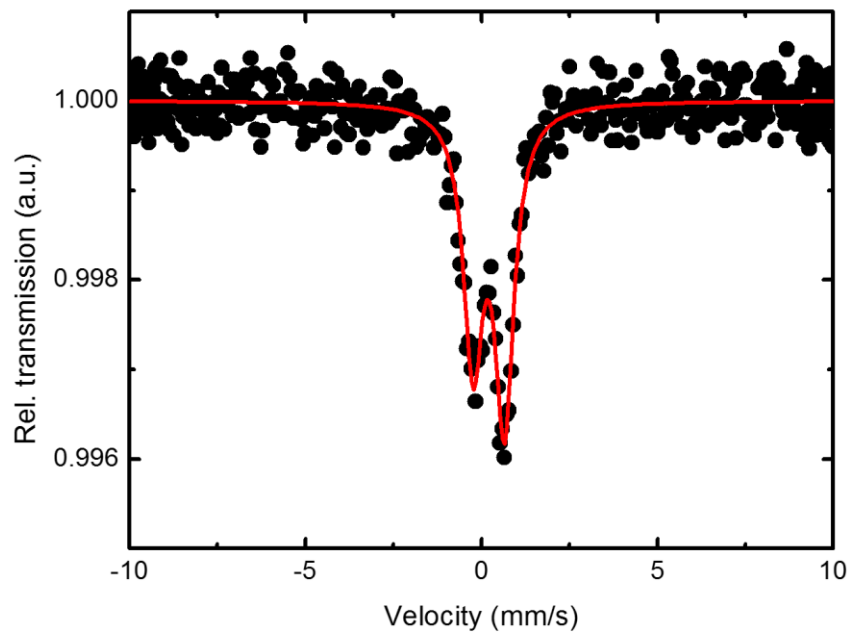
Figure S17. Zero-field Mössbauer spectrum of [Fe(^{DEA}PDI)(NO)$_2$][PF$_6$] (**4**), [δ = 0.308(7); ΔE_Q = 0.89(1) mm/s].
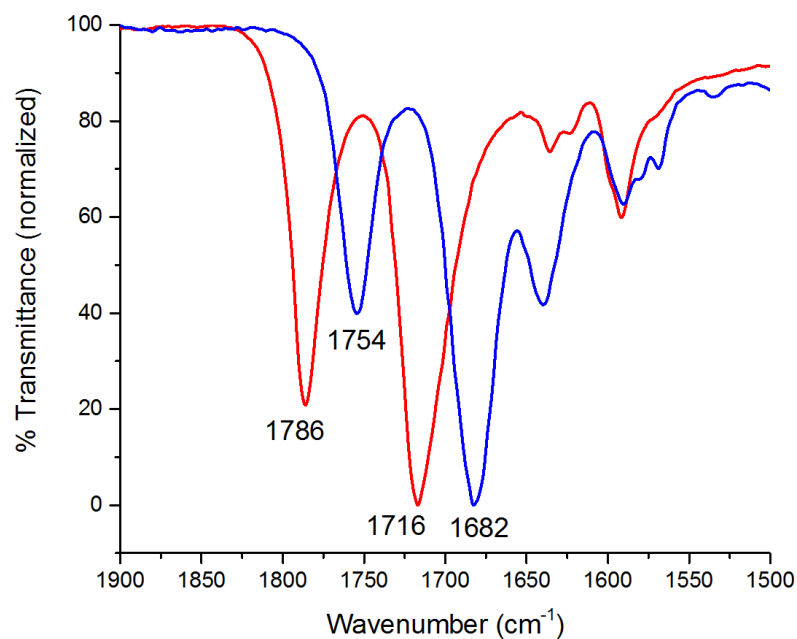
Figure S18. Overlay ATR-FTIR spectra of **4(^{14}NO)$_2$** (red) and **4(^{15}NO)$_2$** (blue).
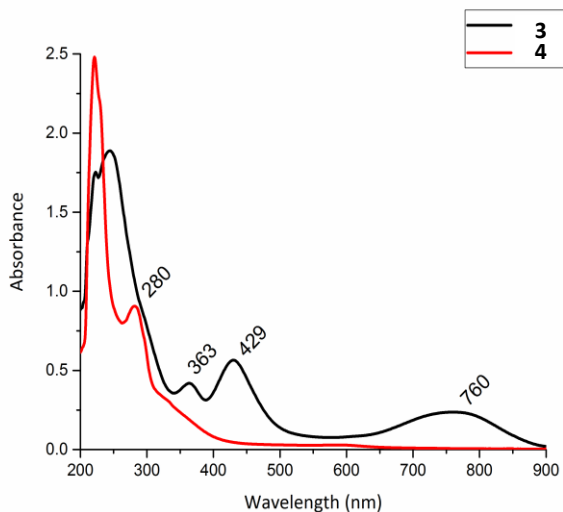
Figure S19. Overlay UV-Vis spectra of $[Fe(H^{DEA}PDI)(CO)_2][PF_6]$ **(3)** (black line) and $[Fe(^{DEA}PDI)(NO)_2][PF_6]$ **(4)** (red line).
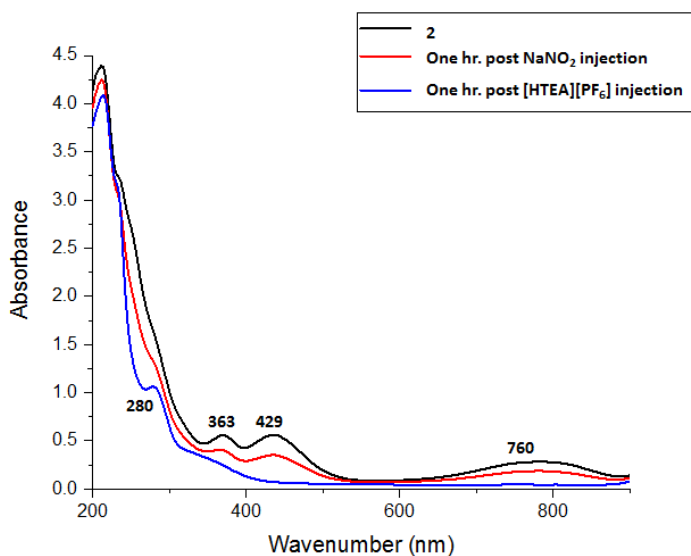
Figure S20. Overlay UV-Vis spectra of $Fe(^{DEA}PDI)(CO)_2$ **(2)** in THF before (black line) and after (red line) stirring with $NaNO_2$ for one hour. The slight decrease in absorbance is due to dilution upon injection of $NaNO_2$ THF/MeOH mixture and doesn't change over the course of one hour. The blue line is one hour after injection of $[HTEA][PF_6]$ demonstrating nitrite reduction.
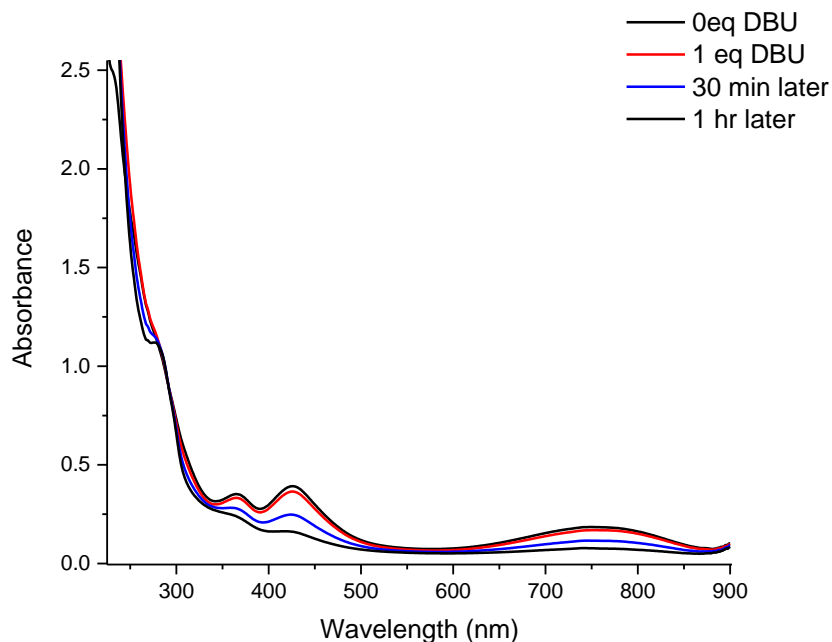
Figure S21. Overlay UV-Vis spectra of Fe(^{DEA}PDI)(CO)$_2$ (**2**) in THF with one equivalent of DBU (pKa = 24.3 in acetonitrile) . The slight decrease in absorbance is due to dilution upon injection of DBU. Decomposition of **2** over one hour results.
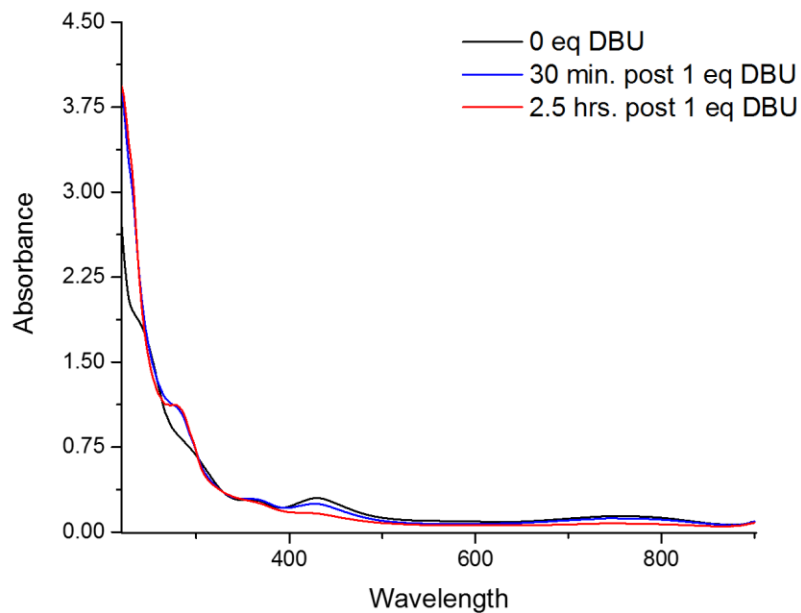
Figure S22. Overlay UV-Vis spectra of [Fe(H^{DEA}PDI)(CO)$_2$][PF$_6$] (**3**) in THF with one equivalent of DBU (pKa = 24.3 in acetonitrile) . The slight decrease in absorbance is due to dilution upon injection of DBU. Decomposition of **3** over two hours results.
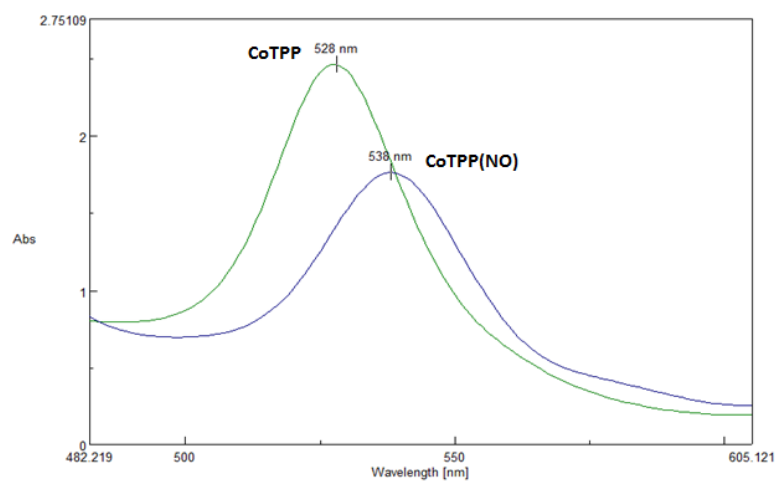
Figure S23. Overlay UV-Vis spectra of pure CoTPP (green) and pure CoTPP(NO) (blue) in THF.
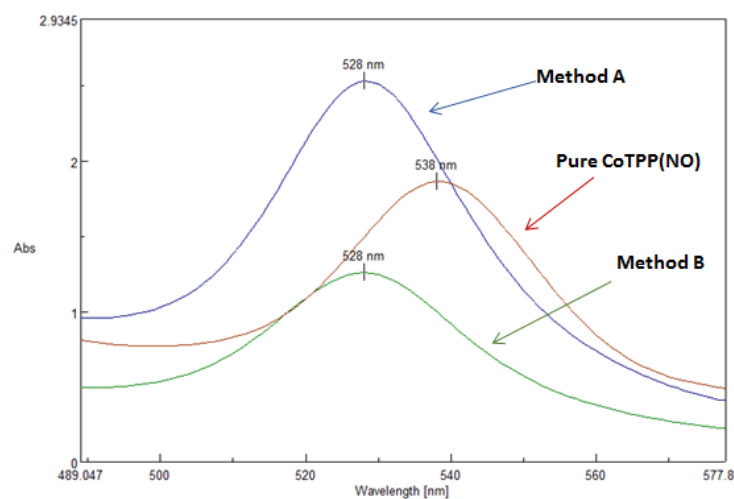
Figure S24. Overlay UV-Vis spectra of [HNEt$_3$][PF$_6$] + NaNO$_2$ reaction utilizing CoTPP probe.
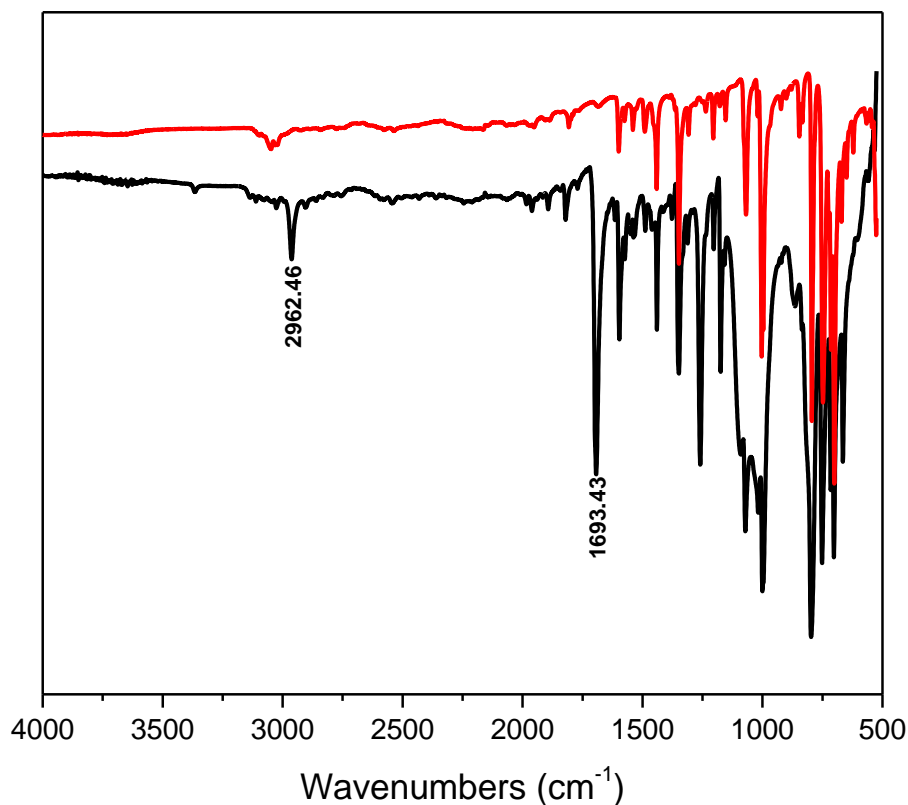
Figure S25. Overlay FTIR spectra of [HNEt₃][PF₆] + NaNO₂ reaction (red) utilizing CoTPP probe and pure CoTPP(NO) (black).
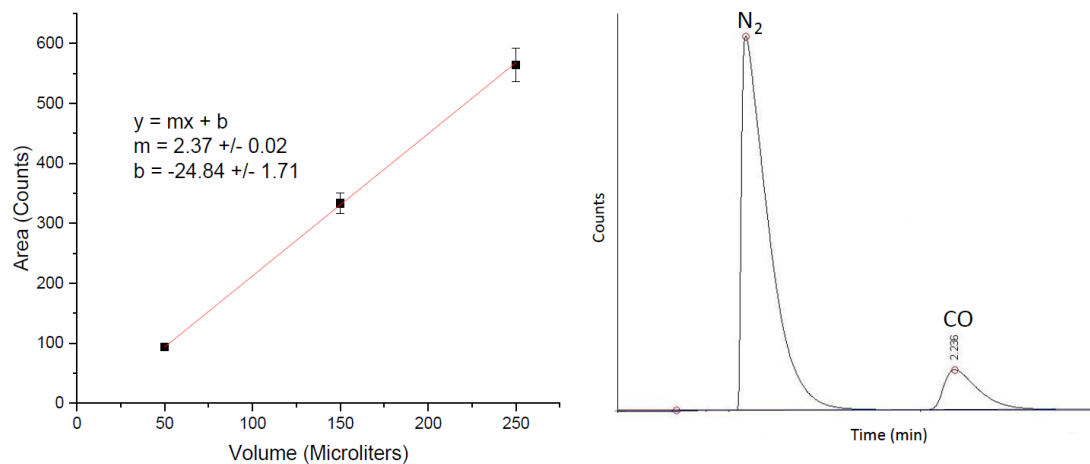
Figure S26. CO gas calibration curve (left) and a representative gas chromatograph of the headspace of the reaction (right) for the reaction of [Fe(H^{DEA}PDI)(CO)₂][PF₆] (**3**) with 1 equivalent of NaNO₂. The area of CO was calculated to be 265.16 counts at a retention time of 2.236 min from a 1 mL injection of a 10 mL headspace = 0.0546 mmol CO, ~40% yield in CO (theoretical value = 0.147 mmol).
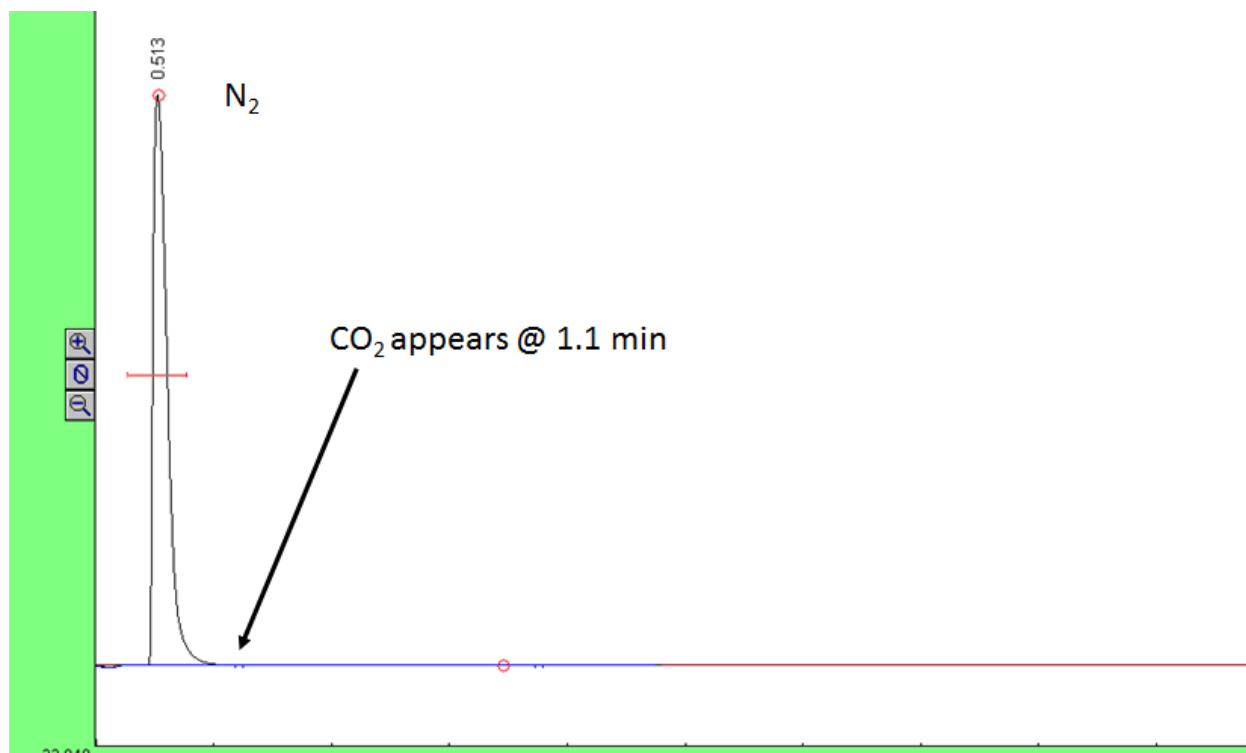
Figure S27. A representative gas chromatograph of the headspace of the reaction for the reaction of $[Fe(H^{DEA}PDI)(CO)_2][PF_6]$ (**3**) with 1 equivalent of $NaNO_2$. The peak at 0.513 min represents N_2. The retention time of CO_2 = 1.18 min, indicating no CO_2 in the headspace.
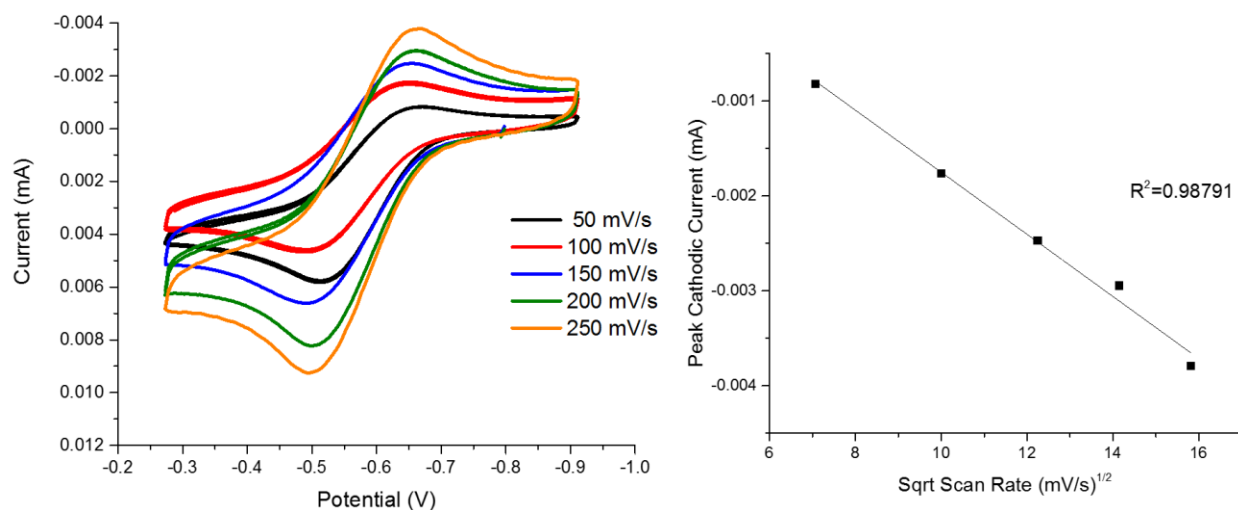
Figure S28. Reversibility study of in 0.001 M Fe(^{DEA}PDI)(CO)$_2$] (**2**) and 0.1 M TBAPF$_6$ in CH$_2$Cl$_2$ of E$_{1/2}$ = - -0.579 V vs. Fc$^{+/0}$ region. Linear fit of cathodic peak currents versus the square root of scan rates is shown.
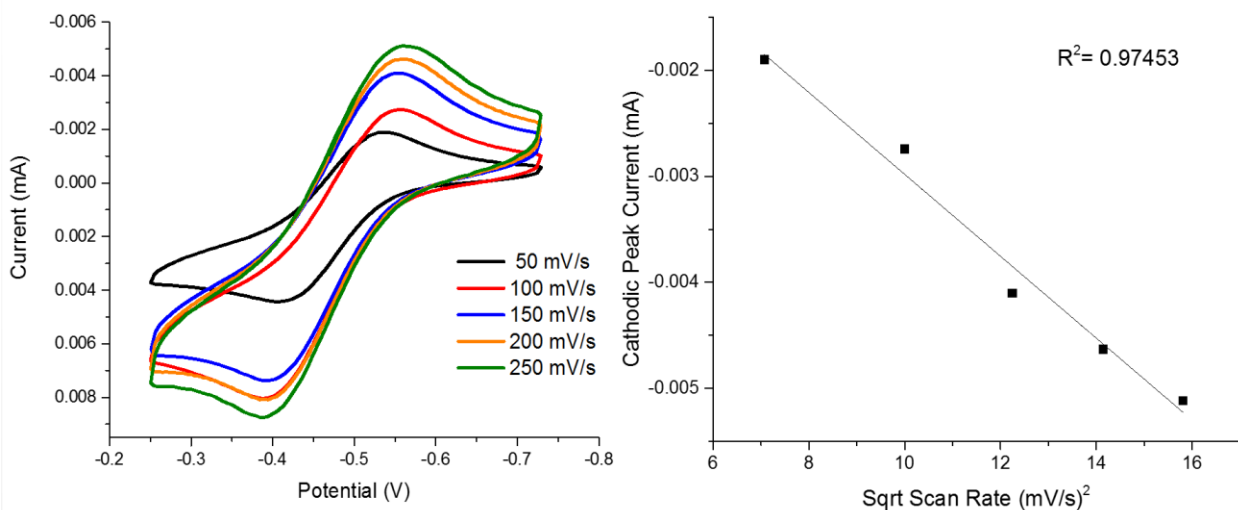
Figure S29. Reversibility study of in 0.001 M [Fe(H^{DEA}PDI)(CO)$_2$][PF$_6$] (**3**) and 0.1 M TBAPF$_6$ in CH$_2$Cl$_2$ of E$_{1/2}$ = -0.474 V vs. Fc$^{+/0}$ region. Linear fit of cathodic peak currents versus the square root of scan rates is shown.
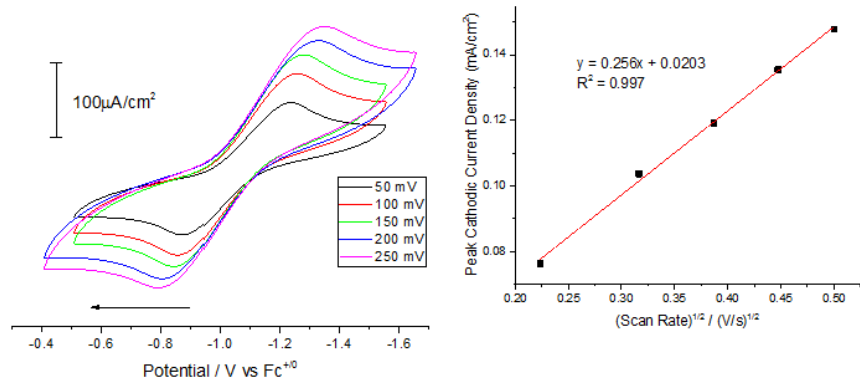
Figure S30. Reversibility study of in 0.001 M [Fe(^{DEA}PDI)(NO)$_2$][PF$_6$] (**4**) and 0.1 M TBAPF$_6$ in CH$_3$CN of E$_{1/2}$ = -1.06 V vs. Fc$^{+/0}$ region. Linear fit of cathodic peak currents versus the square root of scan rates is shown (R^2= 0.997).
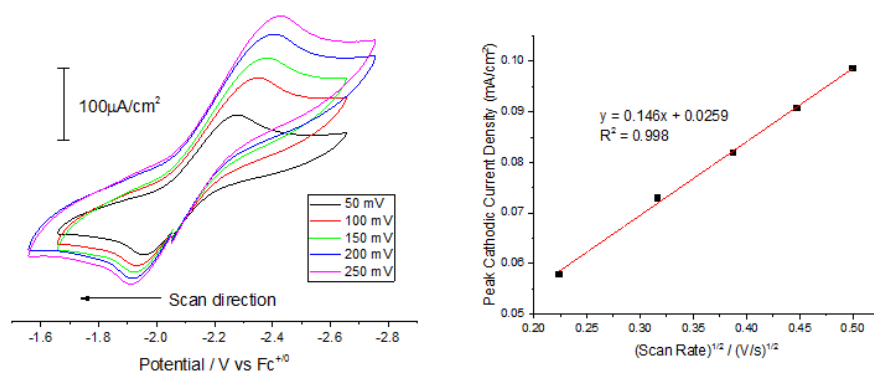
Figure S31. Reversibility study of in 0.001 M [Fe(^{DEA}PDI)(NO)$_2$][PF$_6$] (**4**) and 0.1 M TBAPF$_6$ in CH$_3$CN of E$_{1/2}$ = -2.15 V vs. Fc$^{+/0}$ region. Linear fit of cathodic peak currents versus the square root of scan rates is shown (R^2= 0.998).

Table S1. Spectroscopic and Structural Parameters for Selected Cationic {Fe(NO)$_2$}^{9} DNICs.

Complex	vNO (cm^{-1})	Fe-N(O) (Å)	N-O (Å)	EPR g value	δ (mm/s)	ΔE_Q (mm/s)	ref
[Fe(^{DEA}PDI)(NO)$_2$]$^+$	1786, 1716	1.688	1.173	2.01	0.308(7)	0.89(1)	this work
[Fe(^{iPr}PDI)(NO)$_2$]$^+$	1794, 1721	1.704	1.169	2.01			7
[Fe(dmp)(NO)$_2$]$^+$	1746, 1840	1.674	1.174	2.08, 2.05, 2.00	0.37	1.77	8
[Fe(ar-nacnac)(NO)$_2$]$^+$	1705, 1755	1.688	1.177	2.06	0.19	0.79	9
[Fe(NHC-iPr)$_2$(NO)$_2$]$^+$	1723, 1791	1.696	1.177	2.03	0.11	0.27	10

References:

[1] C. Bianchini, C. G. Mantovani, A. Meli, F. Migliacci, F. Zanobini, F. Laschi and A. Sommazzi, *Eur. J. Inorg. Chem.,* 2003, 1620-1631.

[2] S. K. Sur, *J. Magn. Reson.,* 1988, **82**, 169– 173

[3] G. A. Bain and J. F. Berry, *J. Chem. Educ.,* 2008, **85**, 532– 536.

[4] G. M. Sheldrick, *Bruker/Siemens Area Detector Absorption Correction Program*, Bruker AXS, Madison, WI, 1998.

[5] P. Van der Sluis and A. L. Spek, *Acta Cryst., Sect. A,* 1990, **A46**, 194-201.

[6] G. M. Sheldrick, *Acta Cryst.*, 2008, **A64**, 112-122.

[7] W. Shih, T. Lu, L. Yang, F. Tsai, M. Chiang, J. Lee, Y. Chiang and W. Liaw, *J. Inorg. Biochem*., 2012, **113**, 83-93.

[8] A. L. Speelman, B. Zhang, A. Silakov, K. M. Skodje, E. E. Alp, J. Zhao, M. Y. Hu, E. Kim, C. Krebs and N. Lehnert, *Inorg. Chem.,* 2016, **55**, 5485-5501.

[9] Z. J. Tonzetich, L. H. Do and S. J. Lippard, *J. Am. Chem. Soc*., 2009, **131**, 7964– 7965.

[10] J. L. Hess, C.-H. Hsieh, J. H. Reibenspies and M. Y. Darensbourg, *Inorg. Chem.,* 2011, **50**, 8541– 8552.